

Direct-bonded GaAs/InGaAs tandem solar cell

Katsuaki Tanabe,^{a)} Anna Fontcuberta i Morral,^{b)} and Harry A. Atwater^{b)}
*Thomas J. Watson Laboratory of Applied Physics, California Institute of Technology,
 Pasadena, California 91125*

Daniel J. Aiken
Emcore Photovoltaics, Albuquerque, New Mexico 87123

Mark W. Wanlass
National Renewable Energy Laboratory, Golden, Colorado 80401

(Received 19 March 2006; accepted 26 July 2006; published online 6 September 2006)

A direct-bonded GaAs/InGaAs solar cell is demonstrated. The direct-bonded interconnect between subcells of this two-junction cell enables monolithic interconnection without threading dislocations and planar defects that typically arise during lattice-mismatched epitaxial heterostructure growth. The bonded interface is a metal-free n^+ GaAs/ n^+ InP tunnel junction. The tandem cell open-circuit voltage is approximately the sum of the subcell open-circuit voltages. The internal quantum efficiency is 0.8 for the GaAs subcell compared to 0.9 for an unbonded GaAs subcell near the band gap energy and is 0.7 for both of the InGaAs subcell and an unbonded InGaAs subcell, with bonded and unbonded subcells similar in spectral response. © 2006 American Institute of Physics.

[DOI: [10.1063/1.2347280](https://doi.org/10.1063/1.2347280)]

III-V compound multijunction solar cells enable ultra-high efficiency performance in designs where subcells with high material quality and high internal quantum efficiency can be employed.¹ However, the optimal multijunction cell band gap sequence cannot be achieved using lattice-matched compound semiconductor materials. Most current compound semiconductor solar cell design approaches are focused on either lattice-matched designs or metamorphic growth (i.e., growth with dislocations to accommodate subcell lattice mismatch), which inevitably results in less design flexibility or lower material quality than is desirable.^{2,3} An alternative approach is to employ direct-bonded interconnects between subcells of a multijunction cell, which enables dislocation-free active regions by confining the defect network needed for lattice mismatch accommodation to tunnel junction interfaces.^{4–8} We report here a direct-bond interconnect multijunction solar cell, a two-terminal monolithic GaAs/InGaAs two-junction cell, to demonstrate a proof of principle for the viability of direct wafer bonding for solar cell applications.

Before studying the direct bonding of solar subcells, direct bonding of bulk GaAs and InP wafers was investigated. (001) n -type GaAs and InP wafers doped, respectively, with Si and S were used. The wafers were diced into ~ 1 cm² area and bonded following the procedure described elsewhere.⁸ Special care was taken to keep the surface of the wafers clean of organic contaminations and particles. After degreasing the surface, the native oxide was removed by dipping the GaAs and InP pieces in 7 vol % HCl (aq) and 10 vol % HF (aq), respectively, for 30 s. Then the wafers were brought into contact with the (011) edges aligned. The joined GaAs/InP pairs were annealed at 0.5 MPa at 270 °C in atmosphere for 10 h followed by annealing in 10% H₂ diluted by N₂ (denoted as “H₂/N₂”) or N₂ at 450–600 °C for

30 min. Some bonded pairs were subject to only one of these two annealing processes.

The electrical properties of the bonded interfaces were investigated for the different annealing conditions by measuring the current-voltage (I - V) characteristics. Bonded pairs with both high and low doping concentrations at the subsequent bond interfaces were investigated. In the following, these pairs will be denoted, respectively, as n GaAs/ n InP and n^+ GaAs/ n^+ InP. The doping concentrations for low doped pairs were 2×10^{18} cm⁻³ Si for GaAs and 4.5×10^{18} cm⁻³ S for InP. For pairs denoted as n^+ GaAs/ n^+ InP, the doping concentration was 1×10^{19} cm⁻³ both for GaAs and InP. These high doped layers were prepared by metal organic chemical vapor deposition (MOCVD). Secondary-ion mass spectroscopy (SIMS) depth profile measurements were performed across the bonded interfaces of GaAs/InP to analyze the chemical composition of the bonding interfaces. Cesium ions were used for sputtering to obtain depth profiles of hydrogen and oxygen.

For multijunction solar cells, formation of mechanically robust, low resistance interfaces is a critical aspect for structure stability and high energy conversion efficiency. I - V characteristics were compared among the bonded n GaAs/ n InP pairs with various annealing conditions. Ohmic contact was obtained only for the pair annealed at 0.5 MPa at 270 °C followed by annealing at 600 °C in H₂/N₂, as shown in Fig. 1(a), which indicates a significant effect of hydrogen at high temperature.

Figure 2 depicts the depth profiles of hydrogen and oxygen concentrations across the bonded n GaAs/ n InP heterointerfaces measured by SIMS before and after the annealing in H₂/N₂ at 600 °C. This result shows a significant reduction of the interfacial hydrogen and oxygen following the 600 °C anneal in H₂/N₂. The integrated dose of oxygen after the 600 °C annealing corresponds to a layer with thickness of around 1 nm, which is a reasonable value to induce tunneling current to enable one to obtain Ohmic heterointerfaces, perhaps with some oxide breakdown by the applied

^{a)}Electronic mail: tanabe@caltech.edu

^{b)}Also at Aonex Technologies, Pasadena, CA 91106.

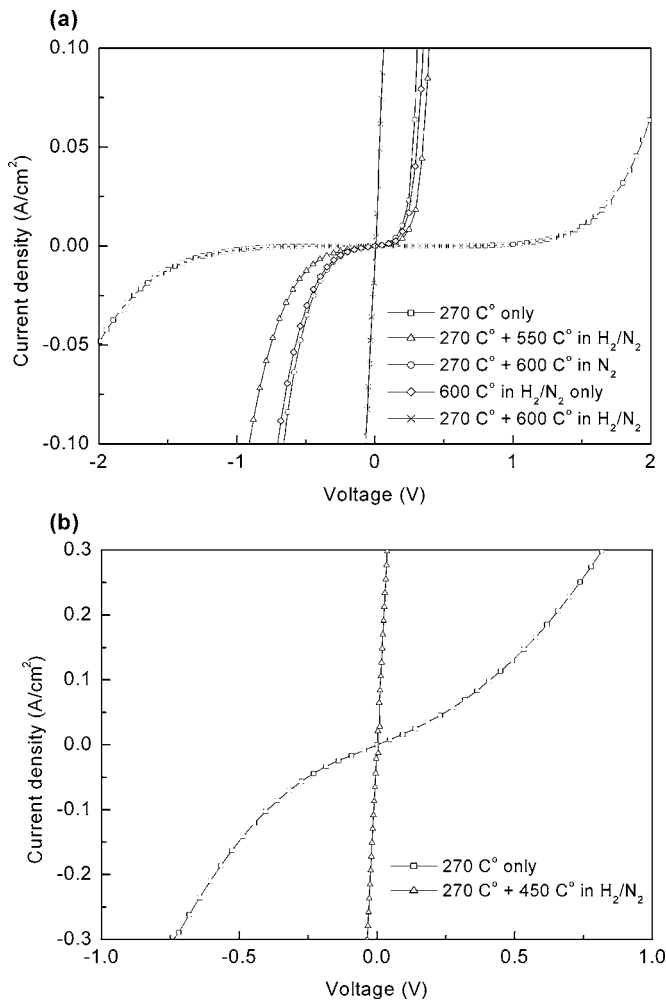


FIG. 1. *I*-*V* characteristics of the bonded GaAs/InP heterointerfaces for (a) *n*GaAs/*n*InP and (b) *n*⁺GaAs/*n*⁺InP. Positive bias voltage was applied from the GaAs side.

voltage.^{9,10} A general picture for the chemical evolution of the bonded bulk GaAs/InP interface could be as follows: Upon room temperature bond initiation, the GaAs/InP interface is characterized mainly by van der Waals bonding. A covalently bonded GaAs/InP interface is subsequently formed in annealing at 270 °C under pressure, mediated by a thin interfacial oxide, as indicated by SIMS analysis. This is supported also by the fact that the interface of the bonded pair has enough strength to endure the shear force applied in the mechanical polishing process for the SIMS measurement. Applied pressure is presumed to increase the interfacial contact area, as omission of an annealing step under pressure resulted in non-Ohmic *I*-*V* characteristics. Higher-temperature annealing in H₂/N₂ reduces hydrogen and oxygen at the bonded interface, leading to higher interfacial conductance.

Heavy doping at the GaAs and InP interfaces to be subsequently bonded was also found to significantly enhance the GaAs/InP interfacial conductivity. Figure 1(b) shows the *I*-*V* curves of the bonded GaAs/InP interfaces for the *n*⁺GaAs/*n*⁺InP pairs after pressure annealing at 270 °C only and pressure annealing at 270 °C followed by annealing in H₂/N₂ at 450 °C. This conductivity enhancement can be explained by the analysis of the heterojunction band offset at the GaAs/InP interface. Electron transport rather than hole transport dominates the current flow in the *n*-type GaAs and

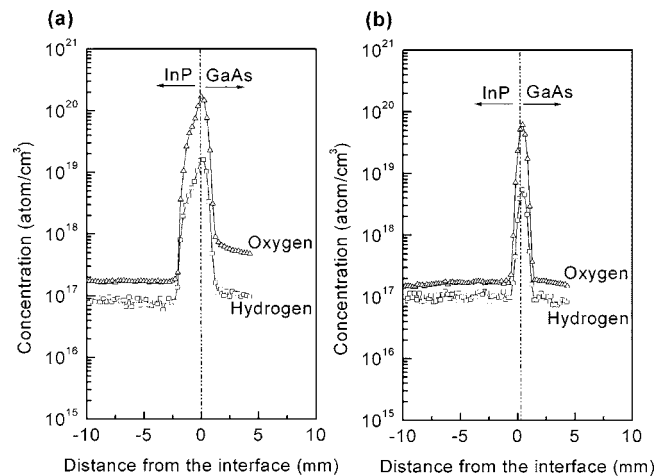


FIG. 2. Elemental concentration profiles across the bonded *n*GaAs/*n*InP heterointerfaces measured by SIMS (a) before and (b) after the annealing in H₂/N₂ at 600 °C. The profiles look extended along the depth than they actually are due to the roughness of the sputtered surface due to the thinning process by mechanical polishing.

InP used in this study. (N.B., the conduction-band edge of GaAs is 0.3 eV above that of InP for intrinsic materials.¹¹) One-dimensional simulations of the heterojunction band bending indicate a significant decrease in the interface potential barrier width at higher doping concentrations, especially on the GaAs side of a GaAs/InP heterojunction.¹² This barrier thinning enables interfacial tunneling, rather than thermionic emission, leading to higher conductivity across the heterojunction interfaces.^{13,14}

Ideally, Ohmic GaAs/InP heterojunctions would be formed by bonding at lower temperature to avoid possible degradation of the cell interfaces and *p*-*n* junctions for multijunction solar cell applications. The approach taken here yielded Ohmic interfaces with 0.12 Ω cm² interface resistance at as low as 450 °C in *n*⁺GaAs/*n*⁺InP structures, as shown in Fig. 1(b).

In the second phase of this study, a two-terminal monolithic, two-junction tandem solar cell was fabricated from direct bonding of single-junction GaAs and InGaAs subcells. The GaAs subcell consisted of *p*- and *n*-type layers of GaAs epitaxially grown on a (001) GaAs substrate by MOCVD. The InGaAs subcell had a band gap energy of 0.74 eV and consisted of *p*- and *n*-type layers of InGaAs layers lattice matched to (001) InP. Specifically, the GaAs subcell was terminated with a Se-doped GaAs layer with 1 × 10¹⁹ cm⁻³ carrier concentration and the InGaAs subcell was terminated with a S-doped InP layer with carrier concentration of 2 × 10¹⁹ cm⁻³. After bonding of the two subcells, the GaAs substrate was removed to complete a GaAs/InGaAs/InP heterostructure forming the two-junction solar cell. The GaAs and InGaAs subcells had *n*-on-*p* structures and the GaAs subcell had a tunnel junction to switch its bottom polarity from *p* type into *n* type for the bonding interface. These subcells were bonded as described above and annealed at 0.5 MPa at 380 °C for 10 h followed by annealing in H₂/N₂ at 350 °C for 30 min after metallization with Au. Photovoltaic *I*-*V* characteristics of the bonded GaAs/InGaAs two-junction cell were measured with 0.337 cm² active illumination area under AM1.5 global solar spectrum with 1 sun total intensity (100 mW cm⁻²). For comparison, photovoltaic *I*-*V* characteristics of the unbonded GaAs and InGaAs subcells

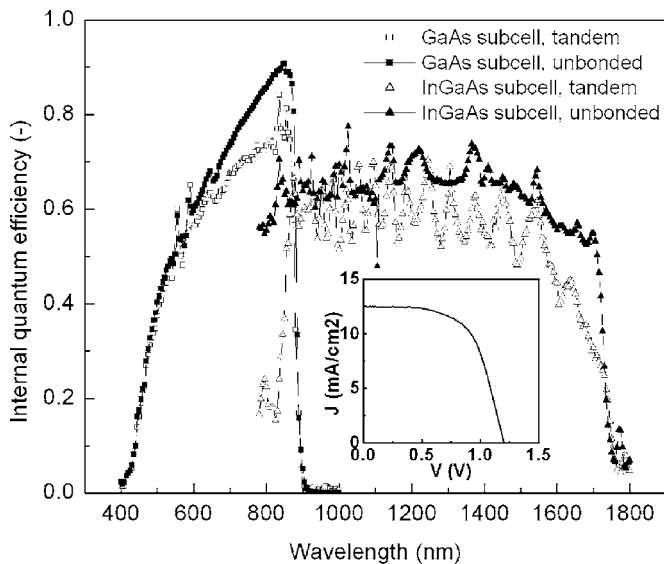


FIG. 3. Spectral response for the bonded GaAs/InGaAs two-junction solar cell and unbonded GaAs and InGaAs subcells and (inset) I - V curve for the bonded GaAs/InGaAs solar cell at 1 sun, AM1.5G.

were also measured. Each of the subcells was processed in the same way as the bonded GaAs/InGaAs cell. The GaAs subcell was mounted on a handling glass substrate with gold film via conductive silver-epoxy glue, for its inversely grown structure, and the original GaAs substrate was removed by chemical etching.

The photovoltaic I - V characteristics of the bonded GaAs/InGaAs two-junction solar cell are shown in Fig. 3 (inset). The device parameters for this cell were $J_{sc}=12.5 \text{ mA cm}^{-2}$, $V_{oc}=1.20 \text{ V}$, $FF=0.62$, and $\eta=9.3\%$, where J_{sc} , V_{oc} , FF , and η are short-circuit current, open-circuit voltage, fill factor, and energy conversion efficiency, respectively. The low fill factor may be accounted for by series resistance in the contacts, which can be lowered by contact redesign. The interfacial resistance for bulk GaAs/InP bonded under the conditions used for the cell was only around 10% of the total series resistance of the cell estimated from the photovoltaic I - V characteristics. The V_{oc} 's of the unbonded GaAs and InGaAs subcells were 0.91 and 0.27 V. Thus, the V_{oc} of the bonded GaAs/InGaAs two-junction cell was approximately equal to the sum of the open-circuit voltages for the GaAs and InGaAs subcells. This V_{oc} result indicates that the bonding process does not degrade the cell material quality since any generated crystal defects that act as recombination centers would reduce V_{oc} .^{15,16} Also, the bonded interface has no significant carrier recombination rate to reduce the open-circuit voltage.

The spectral response for the bonded two-junction cell and unbonded GaAs and InGaAs subcells is given in Fig. 3. The bottom InGaAs subcell as well as the top GaAs subcell of the bonded tandem cell were found to be photovoltaically active. This result indicates a highly transparent bonded GaAs/InGaAs interface. The result of the bonded cell is similar to that of the unbonded subcells in spectral response

and indicates only a small loss of quantum efficiency ($\sim 10\%$) by the cell stacking with direct wafer bonding. The poor quantum efficiency, specifically for the higher energy region, may be caused by a high surface recombination rate at the top surface.¹⁷ Antireflective coating, surface passivation, and optimization of cell assembly parameters, such as metal contacts and current matching, would give further improvement of the cell efficiency.

In this letter we demonstrated the use of direct wafer bonding in a tandem solar cell. Such an approach can also be applied to other photovoltaic heterojunctions where lattice mismatch accommodation is also a challenge, such as the InGaP/GaAs/InGaAsP/InGaAs four-junction tandem cell by bonding a GaAs-based lattice-matched InGaP/GaAs subcell to an InP-based lattice-matched InGaAsP/InGaAs subcell. Simple considerations suggest that for such a cell the currently reported interfacial resistance of $0.12 \text{ } \Omega \text{ cm}^2$ would result in a negligible decrease in overall cell efficiency of $\sim 0.02\%$, under 1 sun illumination.¹⁸

The authors acknowledge Robert Reedy of the National Renewable Energy Laboratory for expert assistance with SIMS measurements. This work was supported by NASA and the National Renewable Energy Laboratory. Alireza Ghaffari, Robert Walters of the California Institute of Technology, and James Zahler of the Aonex Technologies are acknowledged for their technical support in development of the bonding process and the electrical measurements. One of the authors (K.T.) was supported in part by the Japanese ITO Scholarship for International Education Exchange.

¹J. M. Olson, D. J. Friedman, and S. R. Kurtz, in *Handbook of Photovoltaic Science and Engineering*, edited by A. Luque and S. Hegedus (Wiley, New York, 2003), p. 359.

²M. Tachikawa and H. Mori, *Appl. Phys. Lett.* **56**, 2225 (1990).

³Y. Shimizu and Y. Okada, *J. Cryst. Growth* **265**, 99 (2004).

⁴M. Shimbo, K. Furukawa, K. Fukuda, and K. Tanzawa, *J. Appl. Phys.* **60**, 2987 (1986).

⁵Z. L. Liao, *Phys. Rev. B* **55**, 12899 (1997).

⁶U. Goesele and Q. Y. Tong, *Annu. Rev. Mater. Sci.* **28**, 215 (1998).

⁷J. M. Zahler, A. Fontcuberta i Morral, C. G. Ahn, H. A. Atwater, M. W. Wanlass, C. Chu, and P. A. Iles, *Proceedings of the 29th IEEE Photovoltaic Specialists Conference* (IEEE, New York, 2002), p. 45.

⁸A. Fontcuberta i Morral, J. M. Zahler, S. P. Ahrenkiel, M. W. Wanlass, and H. A. Atwater, *Appl. Phys. Lett.* **83**, 5413 (2003).

⁹E. Rosenbaum and L. F. Register, *IEEE Trans. Electron Devices* **44**, 317 (1997).

¹⁰E. Miranda, J. Sune, R. Rodriguez, M. Nafria, and X. Aymerich, *Appl. Phys. Lett.* **73**, 490 (1998).

¹¹S. Tiwari and D. Frank, *Appl. Phys. Lett.* **60**, 630 (1992).

¹²PCID, Version 5.2, University of New South Wales, 1998.

¹³A. Y. C. Yu, *Solid-State Electron.* **13**, 239 (1970).

¹⁴H. Sasaki, L. L. Chang, R. Ludeke, C. Chang, G. A. Sai-Halasz, and L. Esaki, *Appl. Phys. Lett.* **31**, 211 (1977).

¹⁵R. B. Bergmann, *Appl. Phys. A: Mater. Sci. Process.* **69**, 187 (1999).

¹⁶R. Brendel, *Jpn. J. Appl. Phys., Part 1* **40**, 4431 (2001).

¹⁷K. A. Bertness, S. R. Kurtz, D. J. Friedman, A. E. Kibbler, C. Kramer, and J. M. Olson, *Appl. Phys. Lett.* **65**, 989 (1994).

¹⁸P. R. Sharps, M. L. Timmons, J. S. Hills, and J. L. Gray, *Proceedings of the 26th IEEE Photovoltaic Specialists Conference* (IEEE, New York, 1997), p. 895.